Virtual Movement of the Ankle and Subtalar Joints Using Cadaver Surface Models

Movimiento Virtual de las Articulaciones Talocrural y Subtalar Utilizando Modelos de Superficie de Cadáveres

Dong Sun Shin[*] & Min Suk Chung[**]

SUMMARY: Medical students in the dissection room do not fully understand the ankle joint for dorsiflexion and plantar flexion as well as the subtalar joint for inversion and eversion. Thus, a three-dimensional simulation of the movements would be beneficial as a complementary pedagogic tool. The bones and five muscles (tibialis anterior, tibialis posterior, fibularis longus, fibularis brevis, and fibularis tertius) of the left ankle and foot were outlined in serially sectioned cadaver images from the Visible Korean project. The outlines were verified and revised; and were stacked to build surface models using Mimics software. Dorsiflexion and plantar flexion were simulated using the models on Maya to determine the mediolateral axis. Then, inversion and eversion were done to determine the anteroposterior axis. The topographic relationship of the two axes with the five affecting muscles was examined to demonstrate correctness. The models were placed in a PDF file, with which users were capable of mixed display of structures. The stereoscopic image data, developed in this investigation, clearly explain ankle movement. These graphic contents, accompanied by the sectioned images, are expected to facilitate the development of simulation for the medical students' learning and the orthopedic surgeons' clinical trial.

KEY WORDS: Ankle Joint; Subtalar Joint; Visible Human Projects; Computer-Assisted Image Processing; Three-Dimensional Imaging; User-Computer Interface.

INTRODUCTION

The ankle joint (talocrural articulation) is a hinge-type synovial joint, allowing dorsiflexion and plantar flexion in the mediolateral (ML) axis. Inversion and eversion occur along the anteroposterior (AP) axis in the subtalar joint (talocalcaneal joint). The biaxial movements around the talus are induced mainly by five muscles (tibialis anterior, tibialis posterior, fibularis longus, fibularis brevis, and fibularis tertius). Each muscle creates a positional relationship with the ML and AP axes for its own action (Moore *et al.*, 2013).

Medical students observe dry bones and dissected cadavers to understand joint movement. However, they cannot see the topographic anatomy between the axes and associated muscles. Therefore, a three-dimensional (3D) simulation of the ankle movement on the computer would be profitable as an educational tool. Two-dimensional (2D) computed tomography (CT) scans or magnetic resonance images (MRIs) are usually employed as raw data to assemble 3D models, but clinical images are restricted to identify tiny shapes. We have experience building stereoscopic models of various minute structures such as the internal ear from sectioned cadaver images with high resolution and actual body color (Shin *et al.*, 2011, 2012a; Park *et al.*, 2013). In the similar manner, objective models of the ankle structures could also be built and used to understand joint motion.

The purpose of this study was to present teaching contents regarding movement of the ankle and subtalar joints. To achieve the goal, in the serially sectioned images of a male cadaver, bones and muscles of the ankle and foot were outlined and subsequently surface reconstructed. Using the surface models, the joints of concern were virtually moved and observed to determine the location of two joint axes. Additionally, 3D data were collected in a portable document format (PDF) file to enable interactive display.

[*] Department of Orthopaedic Biomaterial Science, Osaka University, Graduate School of Medicine, Osaka, Japan.
[**] Department of Anatomy, Ajou University School of Medicine, Suwon, Republic of Korea.

MATERIAL AND METHOD

Segmentation and surface reconstruction. Sectioned images (intervals 0.2 mm) were acquired from an entire male cadaver (33 years old; statue 1.64 m; weight 55 kg) (Park *et al*., 2005) in the Visible Korean project. We selected 202 images (1 mm intervals) from the distal part of tibia and fibula to the end of foot. The images were opened on Photoshop CS5 version 12 (Adobe Systems, Inc., San Jose, CA, USA) to be saved as Photoshop document files. Our interest was the left-side ankle and foot, beyond which excessive margins were cropped to reduce resolution (3,040 X 2,008) to 992 X 817.

We used the prepared segmented images where the outlines of 33 structures (skin, bones, and muscles) of the left ankle and foot had been drawn (Table I) (Shin *et al*., 2012d). The outlines were placed on the new processed sectioned images and were confirmed and edited if necessary. The outlines were then filled with different colors according to the individual components.

Only color-filled outlines excluding the sectioned images were saved as bitmap (BMP) files. Using Mimics version 17 (Materialise, Leuven, Belgium), 202 BMP files

were placed in a Mimics (MCS) file, and the outlines could be conveniently browsed with a scroll bar. The color-filled outlines were shown together with the coronal and sagittal planes, which were immediately produced by piling all outlines. Vertical planes were displayed by clicking on the horizontal plane or the scroll bar (Fig. 1).

Mimics utilized color brightness to recognize and cluster the serial outlines of every structure. After stacking the categorized colors, all structures were surface reconstructed at the same time. The surface models were painted with the already used colors (Fig. 1).

Faulty outlines gave rise to unexpected steps in the coronal and sagittal planes; the outlines also caused surface models that did not correspond with anatomy. The erroneous outline levels were easily noticed by clicking the defective portion of the vertical plane or model. The outlines were directly amended on Mimics, which allowed manual modification with the "Edit masks" tool. Anatomists corrected the outlines until the secondary images were satisfactory (Fig. 1).

The accumulated outlines in each surface model were removed, and triangular surfaces were appropriately reduced in number. Whole surface models in the MSC file were saved
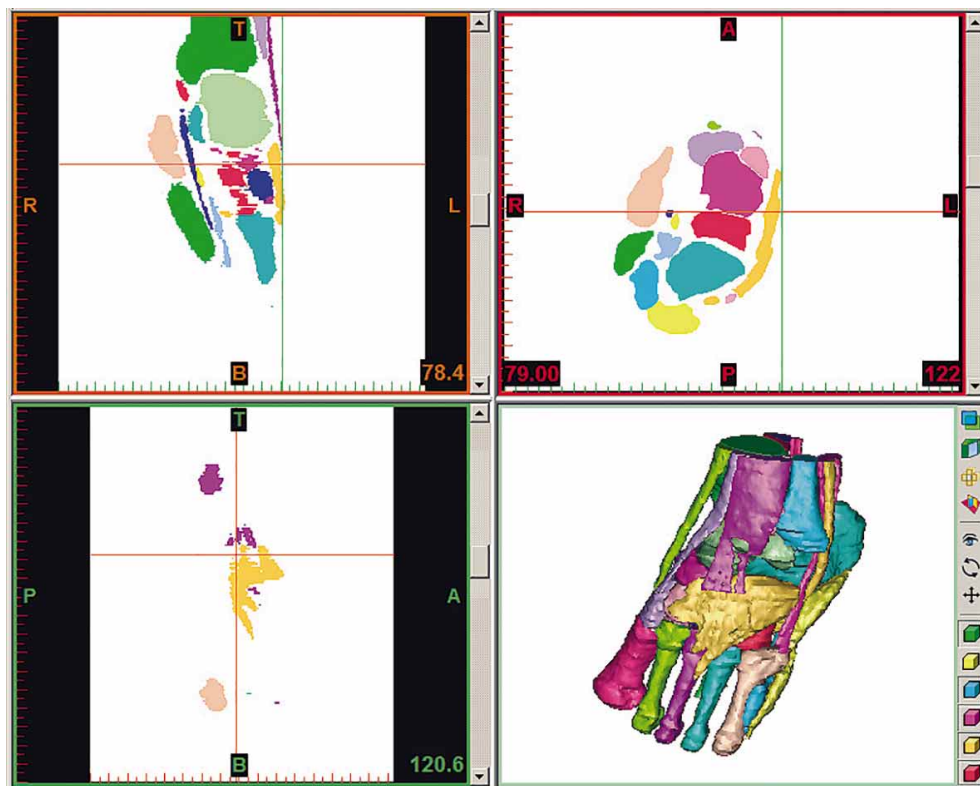

Fig. 1. Mimics file visualizing the original color-filled outlines (top right), accompanied by the coronal plane (top left), sagittal plane (bottom left), and stereoscopic surface models (bottom right).

Table I. Thirty-three structures of the ankle and foot that were outlined and surface reconstructed. (Number of structures).

Systems	Groups	Structures
Integumentary (1)		Skin
Skeletal (27)	Bones of leg (2)	Tibia, Fibula
	Tarsal bones (7)	Talus, Calcaneus, Navicular, Medial cuneiform, Intermediate cuneiform, Lateral cuneiform, Cuboid.
	Metatarsals (5)	1st to 5th metatarsals.
	Phalanges (13)	1st to 5th proximal phalanges, 2nd to 4th middle phalanges, 1st to 5th distal phalanges.
Muscular (5)		Tibialis anterior, Tibialis posterior, Fibularis longus, Fibularis brevis, Fibularis tertius.

as stereolithography (STL) files, which retained the structures' own locational information (Derakhshani, 2012; Naas, 2012; Palamar, 2012).

Virtual movement of joints. The surface models of the bones and five muscles (two tibialis muscles and three fibularis muscles) in the STL format were collected in a Maya binary (MB) file on Maya version 2013 (Autodesk, Inc., San Rafael, CA, USA).

Because the subject had expired in the supine posture, the ankle joints were plantar flexed (Park *et al*., 2005). Thus, the foot bones including the talus were dorsiflexed using the "Animation" function in Maya software to acquire the ankle's anatomical position. During this procedure, the software prevented the bones from overlapping (Palamar). The ML axis

of the ankle joint was manually adjusted until the gap change between the tibia, fibula and the talus was minimized during dorsiflexion. After dorsiflexion, the surrounding muscles were automatically elongated or shortened (Fig. 2).

Virtual movement of the ankle and subtalar joints was attempted from the anatomical position. Further dorsiflexion was simulated along the determined ML axis (Fig. 2). The AP axis was regulated through inversion and eversion of the subtalar joint on the same principle that the interval between the talus and calcaneus did not vary greatly (Fig. 3).

Manufacture of the PDF. Other extrinsic and intrinsic foot muscles (e.g., sole muscles) besides the five mentioned muscles were also delineated in Photoshop and surface reconstructed in Mimics for the PDF file. Individual models
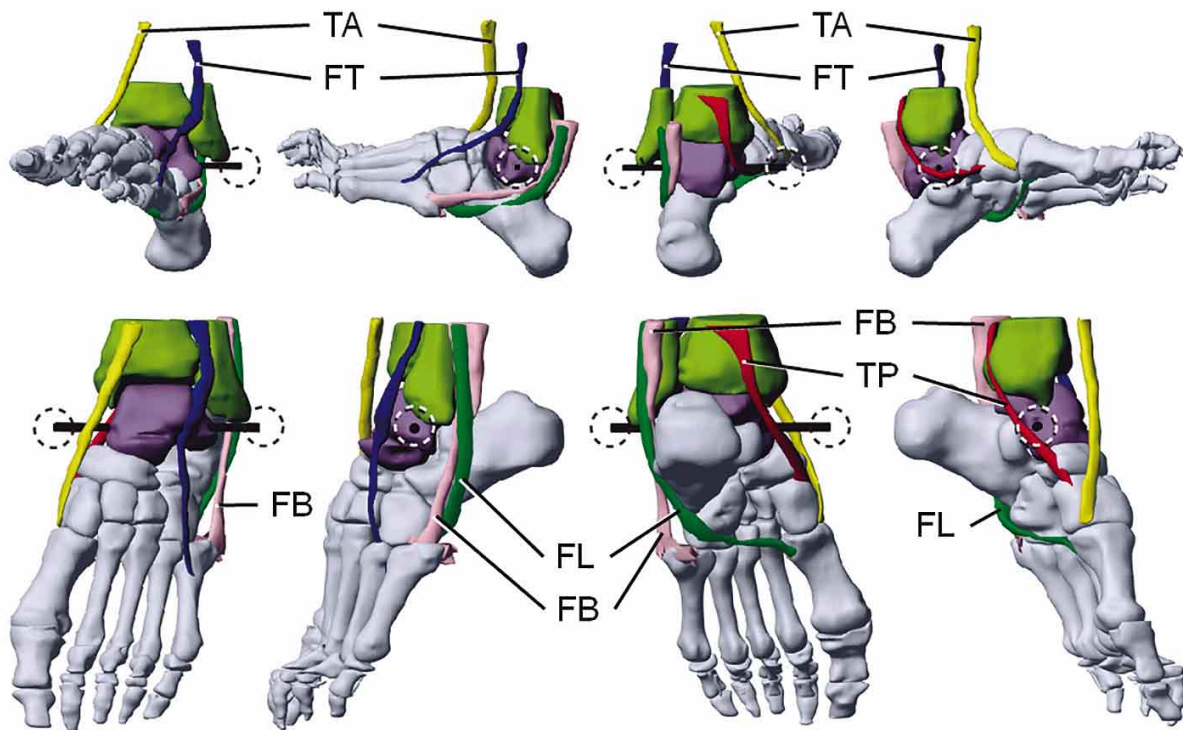

Fig. 2. Simulation of ankle joint movement in the mediolateral axis (dotted circle) in four different views. The surface models are tilted to make the axis look horizontal. Dorsiflexion (top row) is caused by the tibialis anterior (TA) and fibularis tertius (FT), whereas plantar flexion (bottom row) is caused by the tibialis posterior (TP), fibularis longus (FL), and fibularis brevis (FB).
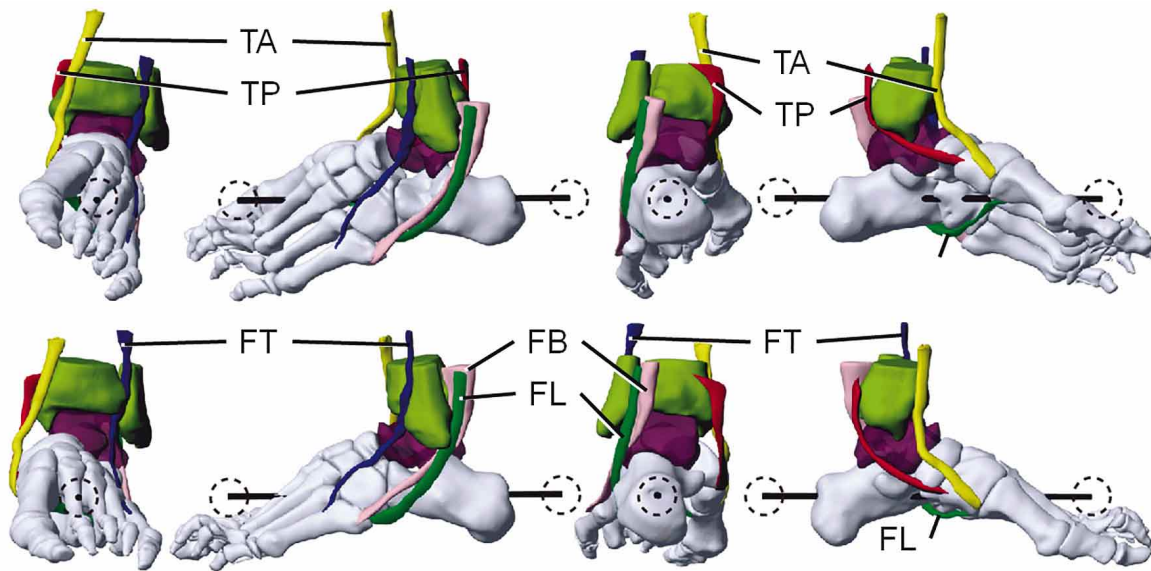
Fig. 3. Simulation of subtalar joint movement in the anteroposterior axis (dotted circle). Inversion (top row) occurs by the tibialis anterior (TA), and tibialis posterior (TP), whereas eversion (bottom row) occurs by the fibularis longus (FL), fibularis brevis (FB), and fibularis tertius (FT).

of the skin, bones, and muscles were saved as STL files (Table I). The surface models and the sectioned images at 2.5 mm intervals were inputted into a PDF file. We employed the inputting method already developed and described in a previous study (Shin *et al*., 2012c).

The notable aspects of this trial were as follows. The ankle was not transformed for anatomical position. The skin color was made semitransparent to show its interior. A goal of bookmark was to demonstrate the five highlighted muscles moving the joints. Another goal was to exhibit stereoscopic labels on the surface models of the five muscles (Fig. 4). Joint motion was recorded in two movies, which were laid in the PDF file (Figs. 2 and 3).

RESULTS

Segmentation and surface reconstruction could be performed concurrently in Mimics. The resulting 3D surface models facilitated verification of the previous delineation of bones and muscles (Fig. 1).

Maya software accomplished virtual movement of the joints. Trial and error yielded an estimate of their axes as follows.

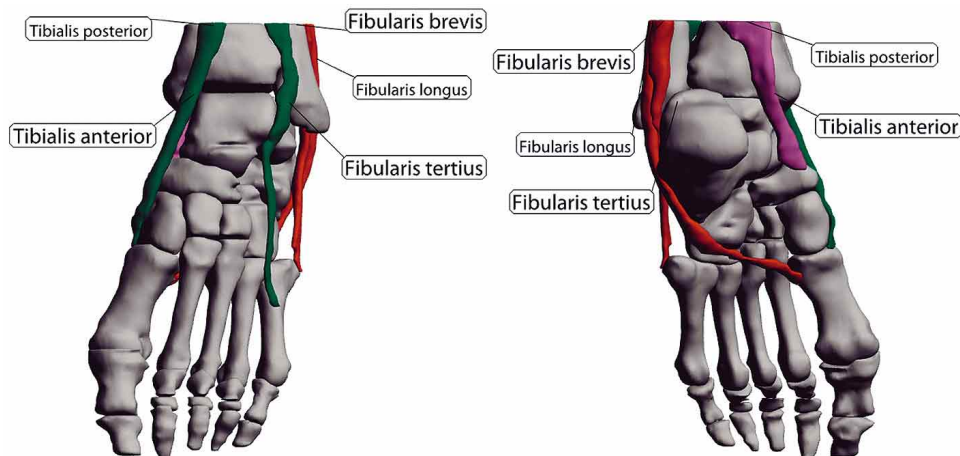The ML axis, passing through the center of the trochlea of talus, was not situated on the horizontal plane

Fig. 4. Annotated surface models of the muscles in the anterior view (left) and posterior view (right).
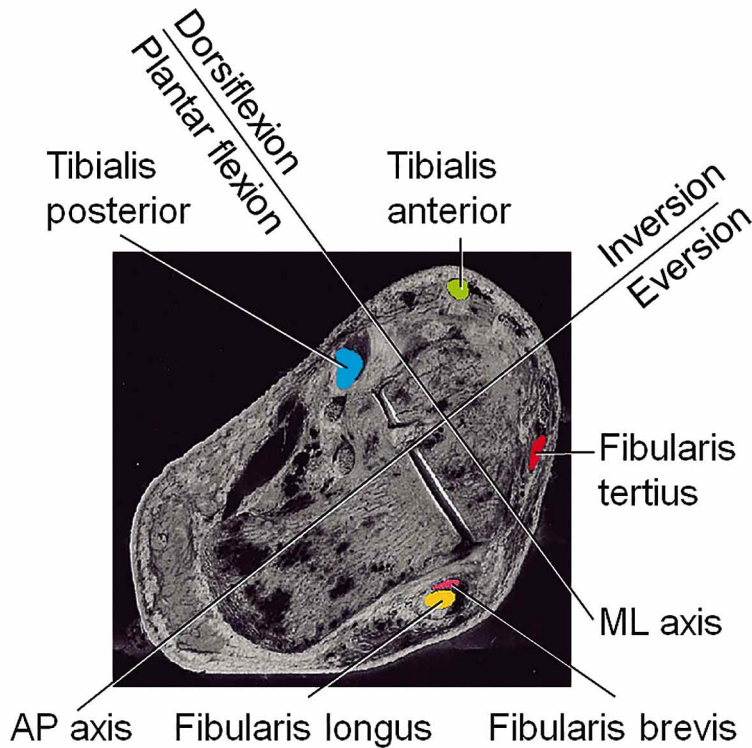
Fig. 5. A horizontal sectioned image where the projected mediolateral (ML) and anteroposterior (AP) axes are drawn. The two axes, almost right-angled, are oblique because the left foot has been laterally rotated. The sectioned image is overlapped with the color-filled outlines of the five muscles.

despite its mediolateral name. The axis was inclined along the direction from medioinferior to laterosuperior, so that the axis was closer to the lateral malleolus and farther from the medial malleolus. As expected, the tibialis anterior and fibularis tertius ran anterior to the ML axis for dorsiflexion, whereas the tibialis posterior, fibularis longus, and fibularis brevis ran posterior to the axis for plantar flexion (Fig. 2).

The AP axis was almost located on the horizontal plane. The axis proceeded from the calcaneal tuberosity to the second metatarsal. The two tibialis (anterior and posterior) passed medial to the AP axis for inversion, but the three fibularis (longus, brevis, and tertius) passed lateral to the axis for eversion (Fig. 3).

The ML and AP axes were projected on a nearby sectioned image, where the five muscles were identified. The illustration showed the expected location of the five muscles with respect to the quadrants created by the two axes. For example, the tibialis anterior for dorsiflexion and inversion was placed in the anteromedial quadrant (Fig. 5).

The PDF file (size 37 MB) is downloadable from the Visible Korean homepage (anatomy.co.kr). Our policy is free downloading and no required registration. Any combinations of the surface models and representative sectioned images can be selected to display and rotated using the PDF file on Adobe Reader version 9 (Fig. 6).

The annotated surface models of the foot muscles, accompanied by the bone models, could be observed; the linkage of the labels and lines with the models was preserved even after rotation (Fig. 4). Supplementary movies on joint motion were displayed by selecting the equivalent page in the PDF file (Figs. 2 and 3).
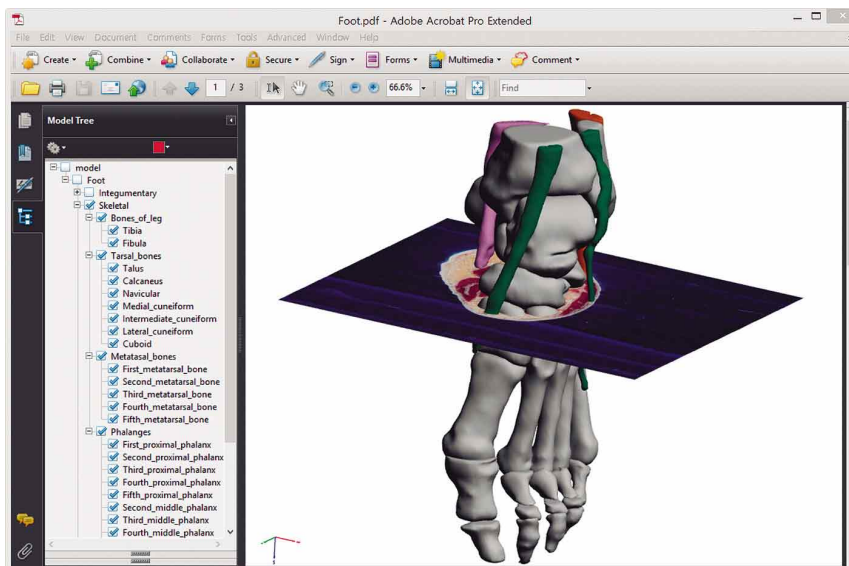

Fig. 6. PDF file consisting of the left model tree window and the right model display window. A sectioned image is superimposed upon the surface models.
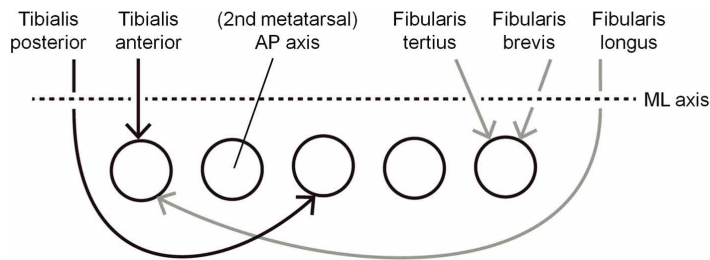
Fig. 7. Schematic illustration of the mediolateral (ML) axis and anteroposterior (AP) axis of the left ankle movements and the five related muscles.

DISCUSSION

The 3D surface models prepared in this study are expected to contribute to the education of ankle and subtalar joints for the reasons.

First, the surface models were made from sectioned images. The high quality sectioned images rather than CTs and MRIs were for the precise surface models. All independent foot muscles were outlined and reconstructed with ease in the previous study (Shin *et al.*, 2012d). The more abundant models of adjoining structures are advantageous for a better simulation. Another merit is that the surface models can be superimposed on the corresponding sectioned images, both of which compensate for each other. The sectioned images provide the surface models with morphological information, and the surface models are the best choice to explain how the 3D structures look in 2D planes (Fig. 6) (Ackerman, 1999; Jastrow & Vollrath, 2003; Heng *et al.*, 2006; Liu *et al.*, 2013).

Second, the surface models can be virtually moved from an anatomist's view point. By moving the ankle and subtalar joints with the articular cavity consistent, reasonable ML and AP axes can be displayed on Maya (Figs. 2 and 3). These surface models correspond to the anatomy knowledge (Moore *et al.*) and will become the source of a virtual exercise system where joints are interactively moved.

Third, the surface models are conveniently browsed in the PDF file. Users are able to generate mixed displays of structures using the check boxes. When a model is clicked, its anatomical name is highlighted in the model tree window. By manipulating the mouse, the surface models can be freely rotated; conveniently zoomed-in, zoomed-out, or shifted. The Adobe Reader toolbar is available for diverse exploration of the surface models (Fig. 6) (Ruthensteiner & Hess, 2008; Kumar *et al.*, 2010; Phelps *et al.*, 2012; Shin *et al.*, 2012b, 2012c, 2013; Kim *et al.*, 2014).

Fourth, the 3D models can be extracted from the PDF file by other researchers. This is a unique characteristic of this product because other software packages do not provide their own raw data. Furthermore, investigators worldwide will be supplied with the full data set including sectioned images, outlined images, and surface models after fulfilling an agreement process with the authors.

The surface models will become more valuable if they are used with a schematic illustration, because the courses of muscles with respect to joint axes are still too complex to be grasped (Fig. 7).

Abduction and adduction of the toes occurs with the standard of the second metatarsal, which is determined by the routes of the dorsal and plantar interossei muscles. Figure 7 shows that inversion and eversion occur with the same standard of the second metatarsal, due to the directions of all five muscles (Moore *et al.*). The latter mechanism is consistent with our result that the AP axis pierces the second metatarsal (Fig. 3). In summary, the second metatarsal is a remarkable guideline for significant foot motions, probably because the skeleton is located in the center of the foot. This is supported by the fact that the third metacarpal in the middle of the hand plays the standard role of the abduction and adduction of fingers.

Joint movements are restricted by ligaments. Therefore, our study would be strengthened by surface models of ankle ligaments. Previously, MRIs of the cadaver ankles were examined to study the ligament morphology (Oh *et al.*, 2006). The sectioned images from the Visible Korean are better for identification and delineation of the ligaments. The subsequent research can be compared with the study of CTs and MRIs of living persons, where real joint movement is observed and analyzed (Lochner *et al.*, 2014). Furthermore, the surface models of ligaments and muscles in the sole might explain not only intrinsic foot motion but also the longitudinal and transverse arches of the foot.

In conclusion, the surface models from cadaver's sectioned images are beneficial for comprehending ankle and foot locomotion. The image data will become a robust resource of virtual dissection for medical students and virtual operation for orthopedic surgeons.

RESUMEN: Los estudiantes de medicina en la sala de disección no entienden completamente la dorsiflexión y flexión plantar de la articulación talocrural, así como la inversión y eversión de la articulación subtalar. Por tanto, la simulación 3D de estos movimientos resultaría beneficiosa como herramienta pedagógica complementaria. Los huesos y cinco músculos (tibial anterior, tibial posterior, fibular largo, fibular corto y fibular tercero), se describen en imágenes del proyecto "Visible Korean", de cadáveres seccionados en serie. Los contornos fueron verificados, revisados, y agrupados para construir modelos de superficie utilizando el programa Mimics. Los movimientos de dorsiflexión y flexión plantar fueron simulados utilizando los modelos generados en el programa Maya, para determinar el eje mediolateral. La inversión y eversión se realizó para determinar el eje anteroposterior. Se examinó la relación topográfica de los dos ejes con los cinco músculos estudiados para demostrar la exactitud de movimientos. Los modelos fueron colocados en un archivo PDF, mediante el cual los usuarios fueron capaces de obtener una visualización combinada de las estructuras. Los datos procedentes de imágenes estereoscópicas, obtenidos en esta investigación, permiten explicar claramente el movimiento de las articualciones talocrural y subtalar. Estos contenidos gráficos, acompañados de las imágenes seccionadas, facilitarán el desarrollo de la simulación en el aprendizaje de los estudiantes y su uso en ensayos clínicos por parte de cirujanos ortopédicos.

PALABRAS CLAVE: Articulación talocrural; Articulación subtalar; Proyecto Humanos visibles; Procesamiento computacional asistido por imágenes; Imágenes tridimensionales; Interface usuario-computador.

REFERENCES

Ackerman, M. J. The Visible Human Project: a resource for education. *Acad. Med., 74(6)*:667-70, 1999.

Derakhshani, D. *Introducing Autodesk Maya 2013.* New Jersey, Sybex/Hoboken, 2012.

Heng, P. A.; Zhang, S. X.; Xie, Y. M.; Wong, T. T.; Chui, Y. P. & Cheng, C. Y. Photorealistic virtual anatomy based on Chinese Visible Human data. *Clin. Anat., 19(3)*:232-9, 2006.

Jastrow, H. & Vollrath, L. Teaching and learning gross anatomy using modern electronic media based on the visible human project. *Clin. Anat., 16(1)*:44-54, 2003.

Kim, B. C.; Chung, M. S.; Kim, H. J.; Park, J. S. & Shin, D. S. Sectioned images and surface models of a cadaver for understanding the deep circumflex iliac artery flap. *J. Craniofac. Surg., 25(2)*:626-9, 2014.

Kumar, P.; Ziegler, A.; Grahn, A.; Hee, C. S. & Ziegler, A. Leaving the structural ivory tower, assisted by interactive 3D PDF. *Trends Biochem. Sci., 35(8)*:419-22, 2010.

Liu, K.; Fang, B.; Wu, Y.; Li, Y.; Jin, J.; Tan, L. & Zhang, S. Anatomical education and surgical simulation based on the Chinese Visible Human: a three-dimensional virtual model of the larynx region. *Anat. Sci. Int., 88(4)*:254-8, 2013.

Lochner, S. J.; Huissoon, J. P. & Bedi, S. S. Development of a patient-specific anatomical foot model from structured light scan data. *Comput. Methods Biomech. Biomed. Engin., 17(11)*:1198-205, 2014.

Moore, K. L.; Agur, A. M. R. & Dalley, A. F. *Clinically Oriented Anatomy.* 7th ed. Philadelphia, Wolters Kluwer/Lippincott Williams & Wilkins, 2013.

Naas, P. *Autodesk Maya 2013 Essentials.* New Jersey, Sybex/Hoboken, 2012.

Oh, C. S.; Won, H. S.; Hur, M. S.; Chung, I. H.; Kim, S.; Suh, J. S. & Sung, K. S. Anatomic variations and MRI of the intermalleolar ligament. *AJR Am. J. Roentgenol., 186(4)*:943-7, 2006.

Palamar, T. *Mastering Autodesk Maya 2013.* New Jersey, Sybex/Hoboken, 2012.

Park, H. S.; Chung, M. S.; Shin, D. S.; Jung, Y. W. & Park, J. S. Accessible and informative sectioned images, color-coded images, and surface models of the ear. *Anat. Rec. (Hoboken), 296(8)*:1180-6, 2013.

Park, J. S.; Chung, M. S.; Hwang, S. B.; Lee, Y. S.; Har, D. H. & Park, H. S. Visible Korean human: improved serially sectioned images of the entire body. *I. E. E. E. Trans. Med. Imaging, 24(3)*:352-60, 2005.

Phelps, A.; Naeger, D. M. & Marcovici, P. Embedding 3D radiology models in portable document format. *A. J. R. Am. J. Roentgenol., 199(6)*:1342-4, 2012.

Ruthensteiner, B. & Hess, M. Embedding 3D models of biological specimens in PDF publications. *Microsc. Res. Tech., 71(11)*:778-86, 2008.

Shin, D. S.; Park, J. S.; Shin, B. S. & Chung, M. S. Surface models of the male urogenital organs built from the Visible Korean using popular software. *Anat. Cell Biol., 44(2)*:151-9, 2011.

Shin, D. S.; Park, J. S. & Chung, M. S. Three types of the serial segmented images suitable for surface reconstruction. *Anat. Cell Biol.,45(2)*:128-35, 2012a.

Shin, D. S.; Jang, H. G.; Park, J. S.; Park, H. S.; Lee, S. & Chung, M. S. Accessible and informative sectioned images and surface models of a cadaver head. *J. Craniofac. Surg., 23(4)*:1176-80, 2012b.

Shin, D. S.; Chung, M. S.; Park, J. S.; Park, H. S.; Lee, S.; Moon, Y. L. & Jang, H. G. Portable document format file showing the surface models of cadaver whole body. *J. Korean Med. Sci., 27(8)*:849-56, 2012c.

Shin, D. S.; Park, J. S.; Park, H. S.; Hwang, S. B. & Chung, M. S. Outlining of the detailed structures in sectioned images from Visible Korean. *Surg. Radiol. Anat., 34(3)*:235-47, 2012d.

Shin, D. S.; Jang, H. G.; Hwang, S. B.; Har, D. H.; Moon, Y. L. & Chung, M. S. Two-dimensional sectioned images and three-dimensional surface models for learning the anatomy of the female pelvis. *Anat. Sci. Educ., 6(5)*:316-23, 2013.

Correspondence to:
Min Suk Chung
Department of Anatomy
Ajou University School of Medicine
164 Worldcup-ro
Suwon 443-380
KOREA

Email: dissect@ajou.ac.kr